Nonlinear buckling instabilities of interspersed railway tracks

Ngamkhanong, Chayut; Kaewunruen, Sakdirat; Baniotopoulos, Charalampos

DOI:
10.1016/j.compstruc.2021.106516

Document Version
Peer reviewed version

Citation for published version (Harvard):
Ngamkhanong, C, Kaewunruen, S & Baniotopoulos, C 2021, 'Nonlinear buckling instabilities of interspersed railway tracks', *Computers & Structures*, vol. 249, 106516. https://doi.org/10.1016/j.compstruc.2021.106516

Nonlinear Buckling Instabilities of Interspersed Railway Tracks

Chayut Ngamkhanong[1,2], Sakdirat Kaewunruen[1,2], and Charalampos Baniotopoulos[1]

[1]Department of Civil Engineering, School of Engineering, University of Birmingham, Birmingham B15 2TT, United Kingdom
cxn649@bham.ac.uk; s.kaewunruen@bham.ac.uk; c.baniotopoulos@bham.ac.uk

[2]Birmingham Centre for Railway Research and Education, School of Engineering, University of Birmingham, Birmingham B15 2TT, United Kingdom

Corresponding author
s.kaewunruen@bham.ac.uk

Abstract

In a conventional railway system, timber sleepers have been widely used for ballasted railway tracks to carry passengers and transport goods. However, due to the limited availability of reliable and high-quality timbers, and restrictions on deforestation the "interspersed" approach is adopted to replace ageing timbers with concrete sleepers. The replacement of ageing timber sleepers is frequently done over old and soft existing formations, which have been in service for so long, by installing new stiff concrete sleepers in their place. This method provides a cost-effective and quick solution for the second and third track classes to maintain track quality. Presently, railway track buckling, caused by extreme temperature, is a serious issue that causes a huge loss of assets in railway systems. The increase in rail temperature can induce a compression force in the continuous welded rail (CWR) and this may cause track buckling when the compression force reaches the buckling strength. According to the buckling evidences seen around the world, buckling usually occurs in ballasted track with timber sleepers and thus there is a clear need to improve the buckling resistance of railway tracks. However, the buckling of interspersed tracks has not been fully studied. This unprecedented study highlights 3D finite element modelling of interspersed railway tracks subjected to temperature change. The effect of the boundary conditions on the buckling shape is investigated. The results show that the interspersed approach may reduce the likelihood of track buckling. The results can be used to predict the buckling temperature and to inspect the conditions of interspersed railway tracks The new findings highlight the buckling phenomena of interspersed railway tracks, which are usually adopted during railway transformations from timber to concrete sleepered tracks in real-life practices globally. The insight into interspersed railway tracks derived from this study will underpin the life cycle design, maintenance, and construction strategies related to the use of concrete sleepers as spot replacement sleepers in ageing railway track systems.

Keywords: interspersed tracks; timber sleeper; concrete sleeper; railway track buckling; interspersed track buckling, snap-through buckling; progressive buckling

1. Introduction

At present, due to the increase in global temperature, track buckling is a serious issue [1-3]. Hence, railway infrastructure developments related to adaptation to future extreme temperature are expected. In railways, high temperature can possibly induce rail buckling, catenary dilatation, signaling and the heating of rolling stock components. As for railway tracks, summer heat can significantly increase the rail temperature and cause the rail to expand, leading to a build-up of axial compression force in continuous welded rail (CWR). Although CWR provides a smooth ride and has a lower maintenance cost, it still suffers from drawbacks as the track tends to be buckled easily when the rail temperature reaches a certain limit [4-7]. Based on the evidence [8-10], track buckling can cause derailment and cause a huge loss of assets and can also result in

the loss of passenger lives. Track buckling around the world usually occurs in conventional railway ballasted tracks with timber sleepers.

Timber railway sleepers have been widely used and are expected to serve for about 15 to 20 years. Due to the limited availability of reliable and high-quality timbers, and restrictions on deforestation, most countries have adopted alternatives to replace ageing timber sleepers [11-13]. Concrete railway sleepers have been widely adopted as the replacement. It is also important to note that the main function of "spot replacement" railway tracks (also called "interspersed railway tracks") is to enhance the performance of the lower-class tracks with low operational speed. These can be found in various countries such as Australia, Japan, the United Kingdom, and the United States [11, 12, 14]. Although a partial replacement of aged and rotten sleepers is obviously more economical than complete track renewal or reconstruction, interspersed tracks have some drawbacks. According to open literature and industry knowledge, this practice could consequently undermine the existing ground foundations and also induce inconsistent local stiffness problems in the rail track system [13, 15-17] and in addition to different track decay rates [18-25]. Studies of interspersed tracks have been carried out [26-29] and it has been found that the replacement of timber sleepers by concrete possibly increase the deterioration rate of the railway track, as uplift behaviour occurs [29].

Previous studies have shown that the buckling strength of ballasted railway tracks depends on the track conditions, track layer geometries, types of elements (fasteners, sleepers, ballast) etc. It is interesting to note that timber and concrete sleepers have different material properties and geometry that lead to the inconsistency in resistance when it comes to interspersed tracks. According to previous studies on track buckling analysis, the major factor, that influences buckling strength, is track lateral resistance. The lateral resistance of tracks consists of sleeper base-ballast friction, sleeper side-ballast friction and ballast shoulder end force. Importantly, different types of sleepers provide different values of lateral resistance and the contribution of lateral resistance of each part is due to their properties [30-36]. It is found that the lateral resistance of timber sleepers is about 60%–80% of that of concrete sleepers. Moreover, maintenance activities, such as ballast tamping, stone blowing, and sleeper replacement, can significantly reduce the compaction of ballast, leading to a reduction in the lateral resistance [32, 33]. Furthermore, torsional resistance also depends on the fasteners and sleeper types. Importantly, the replacement of sleepers should be done carefully since it may severely reduce lateral track stiffness. As seen in many studies on lateral resistance of ballasted tracks, the displacement limit of the lateral force-displacement obtained by STPTs is usually lower than those used in the previous buckling analysis. This implies that previous studies have slightly overestimated the buckling temperature of ballasted tracks. Although track buckling has been widely investigated [37-46], interspersed tracks and their inconsistency have never been fully analysed. The previous study of buckling of interspersed tracks has been preliminary studied using linear analysis and found that the interspersed track can improve the buckling strength of the ageing railway track [47]. However, there is still a need to fully address the benefits of interspersed tracks in buckling prevention.

In this study, the advanced three-dimensional finite element modelling of interspersed railway tracks under various conditions exposed to extreme temperature are presented using LS-DYNA. The simulations are divided into two parts: linear analysis and nonlinear analysis. This paper firstly studies the effects of boundary conditions on buckling temperature and buckling shapes using linear eigenvalue buckling analysis. Secondly, the nonlinear buckling analysis is used considering various parameters that influence the buckling strength. This study applies the values of lateral resistance within the range that possibly buckles the track. The paper thus provides the buckling temperature of interspersed railway tracks under different track conditions. The insights will help track engineers to improve track buckling mitigation methods for conventional ballasted and interspersed railway tracks.

2. The concept of track buckling

If rail temperature is higher than the neutral temperature or stress-free temperature, the compression axial force in the rails builds up. The rail can be buckled when the compression force reaches its limit or buckling

resistance. It should be noted that buckling resistance is affected by track and element types and track conditions. The relationship between rail temperature and lateral displacement is typically plotted as seen in Fig 1. It can be seen that there are two types of buckling depending on the post-buckling path: sudden buckling and progressive buckling. In the pre-buckling stage, the rails are exposed to the temperature over neutral temperature and the axial force is linearly increased. As for the sudden buckling (also called "Snap-through"), the track buckles explosively with no external energy after reaching its maximum temperature (upper critical temperature, T_{Bmax}) and becomes unstable in its post-buckling stages. T_{Bmin} represents the lower bound which can buckle the track if sufficient energy is supplied. It can also be defined as a safe temperature since the track cannot buckle if it experiences a temperature below this temperature. Moreover, progressive buckling can occur when the T_{Bmin} cannot be differentiated from T_{Bmax}. In this case, track lateral displacement is gradually increased after buckling and the critical temperature is defined as T_P.

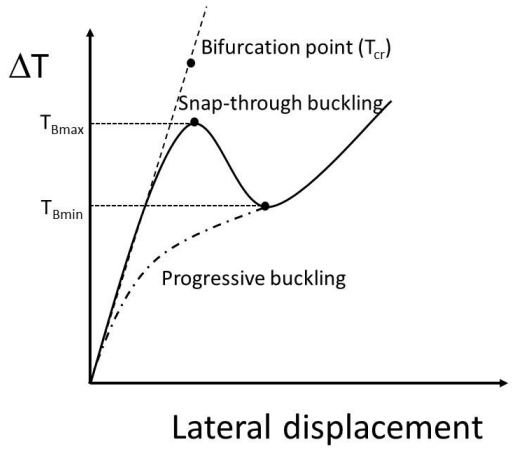

Figure 1 Buckling path.

According to the analytical solutions and buckling shapes observed in the field, there are two main buckling shapes often found: symmetrical and anti-symmetrical shapes. Generally, there are two regions: buckled regions and adjoining regions. The buckled zone is the zone of change in shape of the track geometry in transverse direction, while the rails are deformed longitudinally in the adjoining zone. Fig 2 presents the first symmetrical (Fig 2a) and anti-symmetrical (Fig 2b) shapes and second symmetrical (Fig 2c) and anti-symmetrical (Fig 2d) shapes. The buckled track consists of a buckled region and adjoining region which have a length of *l* and a, respectively. Subscripts 1 and 2 represent the buckled regions 1 and 2. It should be noted that the appropriate nonlinear differential equations governing lateral deflection in the buckled zone and the longitudinal displacement in the adjoining zones are formulated based on large deflection theory [38]. The differential equations are solved to get the resulting equations for different shapes of buckling. For the anti-symmetrical buckling shape, the governing equations are identical to those derived for the symmetrical buckling shape except for the boundary condition. Therefore, the shape of track buckling mostly depends on the boundary conditions which are related to the track conditions in the field.

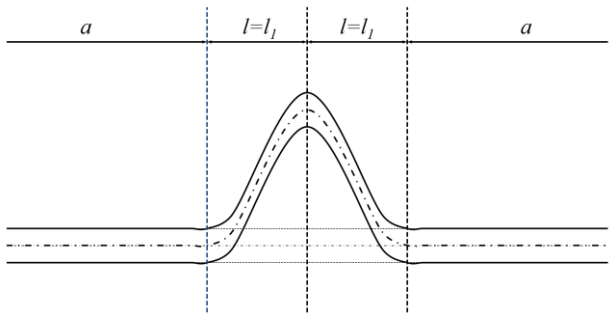

a)

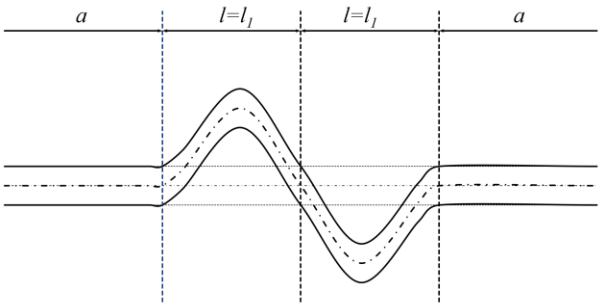

b)

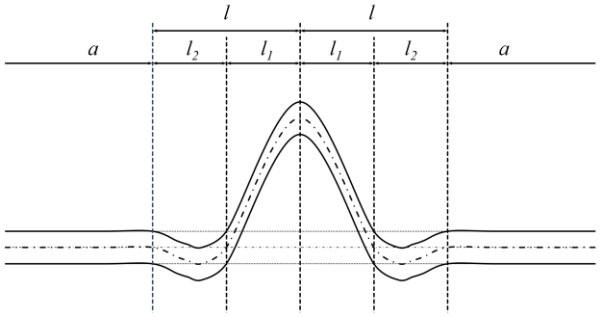

c)

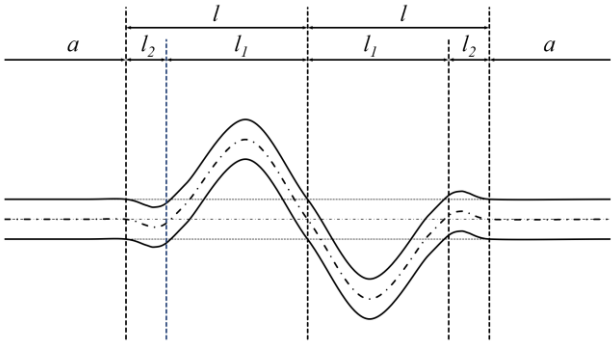

d)

Figure 2 Typical buckling shapes a) symmetrical deformation b) anti-symmetrical deformation c) second symmetrical deformation d) second anti-symmetrical deformation.

3. Modelling

3.1 Finite Element Modelling

In this study, ballasted railway tracks with standard gauge are modelled in LS-DYNA. Steel rails UIC60 and concrete sleepers are modelled as beam elements, which take into account shear and flexural deformations [48]. Rails and sleepers are constructed using SECTION_BEAM and MAT_ELASTIC keywords in LS-DYNA. The MAT_ADD_THERMAL_EXPANSION keyword is assigned to the steel rails to represent the thermal expansion property. The steel rails are connected to the concrete sleepers through the fastener and rail pad which are modelled as the series of spring elements. The rail pads and fasteners are modelled using SECTION_DISCRETE and SPRING_ELASTIC in the connections between the sleepers and the rails. At the rail seat, a rail pad and a fastener, consisting of three translational springs to represent the pad stiffness in three directions and one rotational spring to represent the fastener resistance, are applied. For ballast, the tensionless support spring is considered using user-defined spring property since it allows the beam to life and move over the support while the tensile support is neglected. This presents the realistic behaviour of ballast. The lateral spring of ballast is connected to sleeper ends while the vertical and longitudinal springs are connected to sleepers at rail seats. For track buckling analysis, 60m long ballasted railway tracks are modelled in order to analyse the effects of the temperature rise on the tracks. It should be noted that 60m is long enough to capture track buckling phenomena, and covers the buckling length observed in practice.

The material properties are presented in Table 1. The standard track gauge and rail UIC60 ($A = 76.70\ cm^2$, Mass = 80.21 kg/m, $I_{xx} = 3038.3\ cm^4$ and $I_{yy} = 512.3\ cm^4$) are considered. The lateral resistances of sleepers are based on the initial stiffness within the linear elastic zone obtained from single sleeper (tie) pull/push tests (STPT) that have been carried out by many researchers [30, 31, 49]. The difference in lateral resistance of concrete and timber sleepers have been previously studied. It is known that the lateral resistance ratio between timber track and concrete track is about 0.6–0.8. While the torsional resistance depends on the fastener and sleeper types, it is interesting to note that the conservative torsional stiffness value for timber is greater than that for concrete in general.

Table 1 Material properties.

Parameter list	Characteristic value	Unit
Rail (UIC60)		
Modulus	2×10^5	MPa
Density	7850	kg/m^3
Poisson's ratio	0.25	
Thermal expansion	1.17×10^{-5}	1/C
Concrete sleeper		
Modulus	3.75×10^4	MPa
Shear modulus	1.09×10^4	MPa
Density	2740	kg/m3
Poisson's ratio	0.2	
Lateral stiffness	200-2000	N/mm
Torsional fastening stiffness	75	kNm/rad
Timber sleeper		
Modulus	1.02×10^4	MPa
Shear modulus	3.93×10^3	MPa
Density	1100	kg/m3
Poisson's ratio	0.2	
Lateral stiffness	120-1200	N/mm
Torsional fastening stiffness	225	kNm/rad

In this study, four types of commonly adopted interspersed railway tracks and plain concrete sleepered track are adopted, as shown in Fig 3. They are identified as plain timber railway track ("1 in 1") and "1 in 2", "1 in 3", and "1 in 4" interspersed railway tracks. By definition, "1 in 2" entails the establishment of alternating concrete and timber railway sleepers on the railway tracks, while "1 in 3" refers to another type of interspersed track where one concrete sleeper is seated alongside every two timber sleepers. Similarly, the "1 in 4" configuration indicates that one concrete sleeper is presented for every three timber sleepers along the railway track. It should be noted that a concrete sleepered track is also compared with the timber sleepered and interspersed tracks in this study.

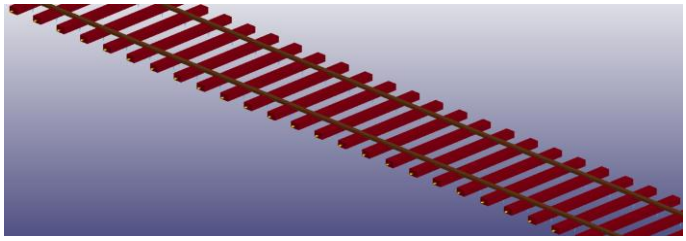

a)

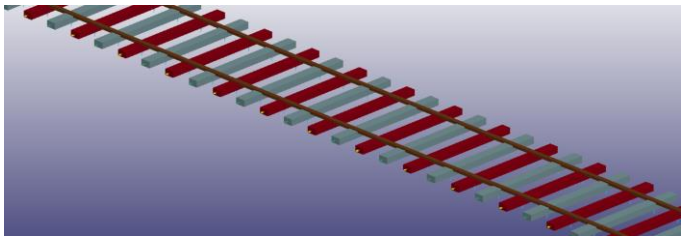

b)

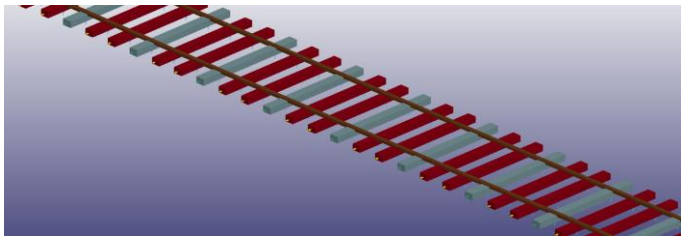

c)

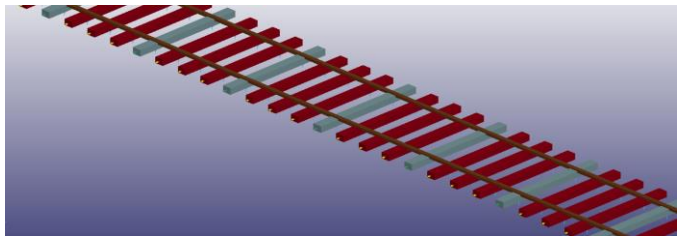

d)

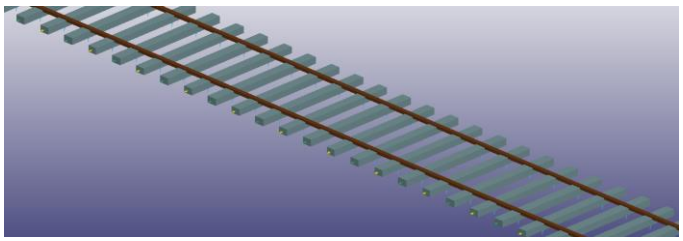

e)

Figure 3 Railway track models: a) timber sleepered track b) "1in2" interspersed track c) "1in3" interspersed track d) "1in4" interspersed track e) concrete sleepered track.

3.2 Boundary conditions

In actual track, there are two regions in buckled track: buckled regions (positive and negative lateral displacement) and adjoining regions. Due to the extreme temperature, the large lateral displacement of rails normally occurs in a transverse direction if the tracks have imperfections, and the rails are deformed longitudinally in adjoining region. It is noted that the buckling shapes of a track are often in symmetrical or anti-symmetrical shapes. Note that, the buckling shape and buckling length in actual track can be changed due to the different track conditions. It is important to note that the buckled region is normally in a weaker zone of track or unconstrained length in this case. The fixed end supports (D_x, D_y, D_z, R_x, R_y, R_z) are applied to the end nodes of the rails. The roller supports (D_x, D_z, R_x, R_y) are applied on the rails to generate the stiff track area so that the rails are constrained and not allowed to move transversally. Hence, the unconstrained length is presented as weaker track and thus this area is expected to buckle. In this study, the track is originally made of 60m length and sufficient for track buckling analysis. As observed in the field, buckling length is normally less than 30m, so the largest unconstrained length of 30m is chosen, while beyond this length is considered as the adjoining zone. The boundary conditions of track models are presented in Fig 4. In this study, the unconstrained length first starts from 6m and is increased to 12m, 18m, 24m, and 30m, respectively. In linear analysis, the rails are assumed to be straight. However, in fact, rails are never perfectly straight and always have imperfections. Hence, the first buckling shape derived from linear analysis is applied as an initial condition in nonlinear analysis.

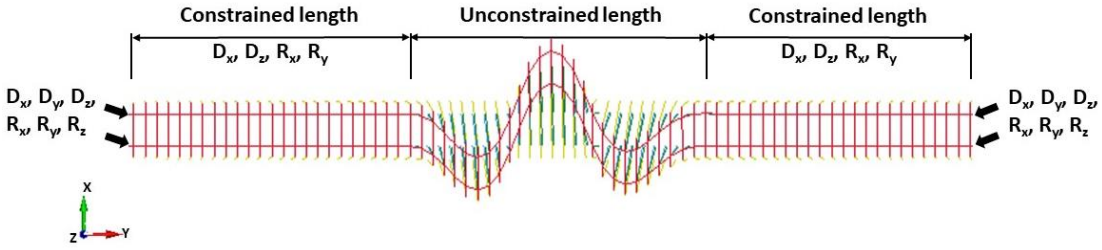

Figure 4 Boundary conditions.

4. Methodology

The study can be divided into two parts: linear Eigenvalue analysis and nonlinear explicit analysis. Linear eigenvalue analysis is first used to predict and analyse the buckling temperature at bifurcation point and corresponding buckling shapes. This section considers the effects of unconstrained length, ballast lateral stiffness and fastener torsional stiffness on buckling shapes. However, it only considers the pre-buckling stage. The optimal unconstrained length is analysed for use in nonlinear analysis. After that, nonlinear explicit analysis is used to capture all stages including pre- and post-buckling. The misalignment amplitudes are taken into consideration to trigger the lateral force in rails. The temperature of 200 °C is applied to the system using the keyword LOAD_THERMAL_LOAD_CURVE in LS-DYNA. The thermal expansion is applied to the rails using the keyword MAT_ADD_THERMAL_EXPANSION.

4.1 Linear Eigenvalue buckling analysis

In linear buckling analysis, the buckling temperature and corresponding mode shapes for railway track can be calculated using an implicit buckle keyword in LS-DYNA based on eigenvalue and eigenvector. It is important to note that the nonlinear properties are not allowed to be used to eigenvalue analysis so that the resistance curve applied to the normal spring (compression and tension) is assumed to be linear, however,

the stiffness values presented are adjusted to comply with the actual spring with tensionless property reflecting the realistic stiffness value. This section analyses that BLF, which is an indicator of the safety factor or the proportion of the given load, is analysed. This factor is then multiplied by the given load to compute the buckling temperature. The buckling modes are computed using Block Shift and Invert Lanczos. The buckling temperature is calculated based on the bifurcation point which is the intersection between the primary and secondary (post-buckling) loads path at which the structure becomes unstable. This can occur at more than one equilibrium position at this point [50, 51]. The post-buckling state does not follow the primary path. In this stage, the secondary slope can be either positive (post-buckling strength) or negative (simply collapse). It should be noted that the stresses are directly proportional to the load factor before reaching the bifurcation point. However, buckling analysis cannot include the nonlinearities and initial imperfection of structure. The governing equation used for calculating the buckling temperature and corresponding buckling shapes is shown in Equation (1).

$$\left|K + \lambda K_g\right| = 0 \tag{1}$$

This equation is equivalent to the eigenvalue solution as shown in Equation (2):

$$Kx = -\lambda K_g x \tag{2}$$

where K is the global stiffness matrix, x is buckling mode vectors, λ is the buckling load factor (BLF), and K_g is a global geometric stiffness matrix known as the initial stress stiffness matrix depending on the stress level of the element. It is noted that the element force vector at each state changes the geometric stiffness of the element.

It is important to note that the buckling load factor (BLF) is an indicator of the safety factor (FOS) against buckling or the ratio of the buckling load to the applied loads. By using Equation (2), the BLFs are calculated and then multiplied by the applied temperature to get the buckling temperature. It should be noted that buckling is predicted when the applied thermal loads are higher than the estimated critical loads (BLF < 1). On the other hand, the track is not buckled under the applied temperature when the BLF is beyond 1. However, linear eigenvalue analysis can still calculate the buckling temperature by extrapolating to reach the buckling temperature, even though the possible buckling temperature is higher than the applied temperature.

4.2 Nonlinear buckling analysis

In nonlinear buckling analysis, the solution method uses the nonlinear with BGFS quasi newton algorithm in LS-DYNA. This iterative method is for solving unconstrained nonlinear optimisation problems. This approach is more accurate than linear analysis since it includes the nonlinearities and covers both pre- and post-buckling of a structure. However, it has been studied that structure without imperfections. theoretically cannot be buckled due to its incompatibility to the solver. It should be noted that perfectly straight tracks remain straight even when they are exposed to extreme temperature and should theoretically buckle. Hence, the initial track imperfection needs to be applied to generate the initial lateral follower force in the rails. It should be noted that initial misalignments are usually seen in the field because of the incorrect stress adjustment, loss of track geometry, loss of lateral resistance etc. This can trigger the lateral force in rails leading to larger misalignment and possible track buckling. The shape of initial misalignment is based on the first fundamental buckling shape that is analysed in linear eigenvalue analysis. The initial misalignments of between 8 and 32m are applied on the rails at mid-tracks. It should be noted that the allowable misalignment can be up to over 30mm depending on class of track [52, 53].

It is noted that, based on previous STPTs on ballast lateral resistance, the load-displacement curves are likely to be bi-linear. Thus, the elastoplastic curve is applied to the lateral spring connected to the sleeper ends to create the lateral resistance of the track. The elastoplastic curve of tensionless spring is presented in Fig 5 where F_p represents the peak force limit and W_p represents the displacement limit. The keyword used in LS-DYNA is MAT_SPRING_INELASTIC with the consideration of tension only. This study

presents two cases (1mm and 2mm) of yielding displacement of ballast. The lateral resistance is presented as the initial stiffness which is the peak lateral force over displacement limit. The temperature is applied LOAD_THERMAL_LOAD_CURVE by applying the temperature (200 °C) load curve with respect to the time domain that has been optimised to avoid the convergence and computational time issues.

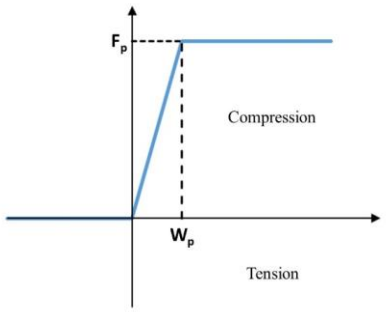

Figure 5 Elastoplastic curve for ballast tensionless spring.

A parametric study is carried out to investigate the effects of various parameters on the buckling temperature of railway ballasted track. The following parameters are taken into account in this study:

- Lateral ballast stiffness (Initial stiffness):
  - 120-1200N/mm for timber sleepers
  - 200-2000N/mm for concrete sleepers
- Lateral ballast peak displacement limit (W_P): 1 and 2mm
- Fastening torsional stiffness:
  - 112.5, 225 (Nominal value), 337.5kNm/rad for timber sleepers
  - 37.5, 75.0 (Nominal value), 112.5kNm/rad for concrete sleepers
- Initial track misalignment (imperfection): 8-32mm.

4.3 Model validation

The models used in this study have been previously used to analyse the vertical responses of interspersed tracks under moving train loads. The results have been validated using experimental parameters, field data, and previous laboratory results [26, 29]. However, interspersed railway track buckling has never been investigated and field data on interspersed track is limited, so the validation of a plain concrete sleepered track is considered. It is noted that a straight ballasted track with only concrete sleepers is considered for validation. Lateral stiffness of 200N/mm and torsional stiffness of 75kNm/rad are considered to compare with the previous studies as these values represent similar track conditions and properties. The result is validated against two different previous analytical solutions and the Finite Element Method (FEM). The analytical solutions are based on the principle of the virtual displacement equation and bending beam theory. The results are solved by assuming the buckling shape and applying the chosen track parameters to the equation. The buckling temperature is then calculated from the corresponding value of axial force [37, 39]. The previous finite element approach used an indirect method combining two rails into one idealised continuous beam with four springs representing the ballast and fastening with spacing of 1 m along the beam [43]. Another model of interspersed tracks constructed in STRAND7 is also compared to the current model in this study [47]. Table 2 presents a comparison between previous studies and the current study. It is found that the result obtained in this study is within the acceptable range of previous studies as the percentage difference of buckling temperature of example model is less than 10% and thus the models can be further used.

Table 2 Buckling temperatures for model validation (°C).

Case	Analytical solutions		FEM		Average	This study	Difference (%)
	[37]	[39]	[43]	[47]			
Torsional stiffness = 75 kNm/rad	57.7	47.8	50.0	53.0	52.1	54.1	3.7

5. Results and Discussion

5.1 Linear analysis

In this section, the unconstrained length represents the weaker area of track where the buckling is expected while the area beyond unconstrained length demonstrates the stiffer area representing better track conditions. Five cases of unconstrained length are considered to understand the physical nature of track buckling. The first global buckling mode of railway tracks considering the lateral stiffness of 200N/mm and 2000N/mm are presented in Fig 6. It can be seen that the buckling shapes of all track types tend to have quite similar shapes if tracks have low lateral stiffness.

The first symmetrical buckling shape is observed in the tracks with 6m unconstrained length and 200N/mm lateral stiffness, as seen in Fig 6a. Whereas the first anti-symmetrical buckling shape can be seen in the all track types with 6m unconstrained length and 2000N/mm lateral stiffness (Fig 6b) and those with 12m unconstrained length and 200N/mm (Fig 6c). In case of 2000N/mm lateral stiffness, concrete sleepered track is likely to have a larger number of buckled regions than other types.

Moreover, the buckling shapes are changed by either increasing or reducing track lateral resistance. The number of buckling regions tends to be increased when the unconstrained length is increased. Hence, based on the analytical solution, the shape of buckling depends on the boundary conditions and lateral stiffness. It is interesting to note that although lateral stiffness can potentially increase the buckling strength and buckling temperature, the buckling shape of a track with higher lateral stiffness tends to have more buckled regions and greater complexity than that of a track with lower lateral stiffness as the track is buckled due to the higher axial compression force.

Interestingly, the buckling shapes of plain tracks can experience more periodic waves than those of interspersed tracks with the same track conditions. It can be concluded that the buckling waveform largely depends on the lateral stiffness and its stiffness inconsistency. However, the amplitude of buckling displacement does not depend on the stiffness inconsistency and the actual magnitude cannot be provided in linear analysis. It should be noted that in the model, the ballast springs are connected in parallel to the sleepers, so that a greater number of concrete sleepers represents higher track lateral stiffness.

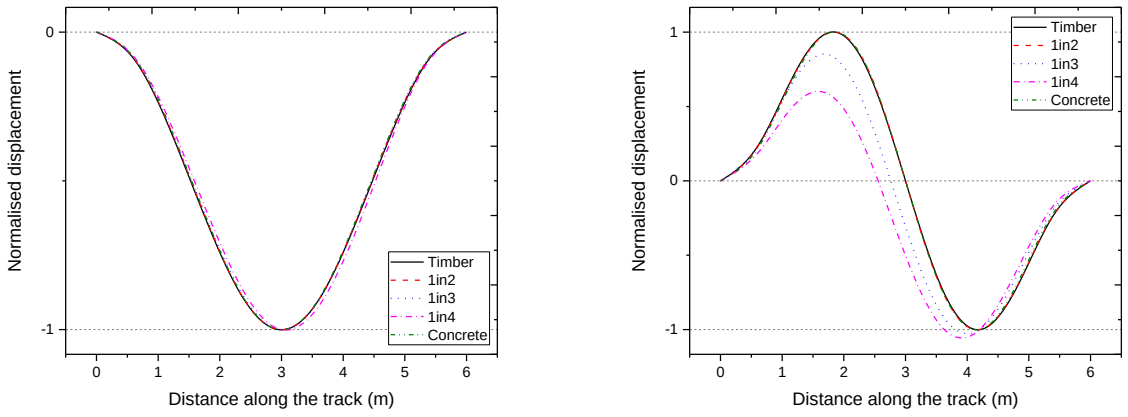

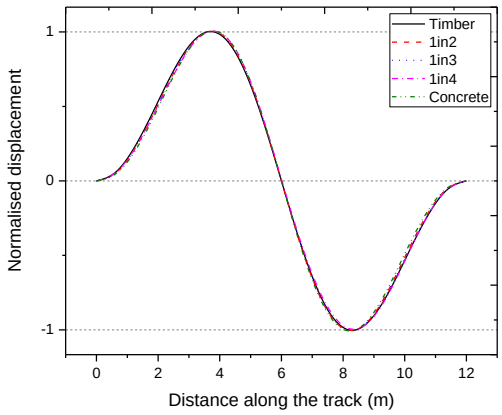
Timber
1in2
1in3
1in4
Concrete
Normalised displacement
Distance along the track (m)

c)

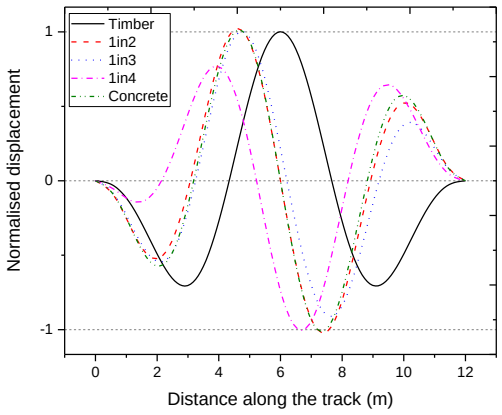
Timber
1in2
1in3
1in4
Concrete
Normalised displacement
Distance along the track (m)

d)

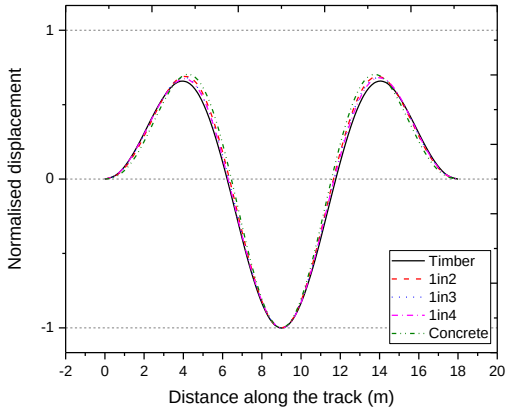
Timber
1in2
1in3
1in4
Concrete
Normalised displacement
Distance along the track (m)

e)

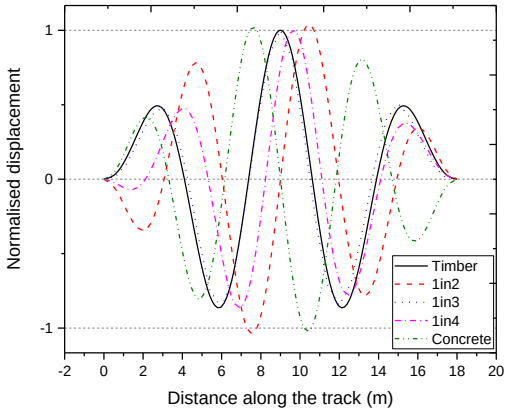
Timber
1in2
1in3
1in4
Concrete
Normalised displacement
Distance along the track (m)

f)

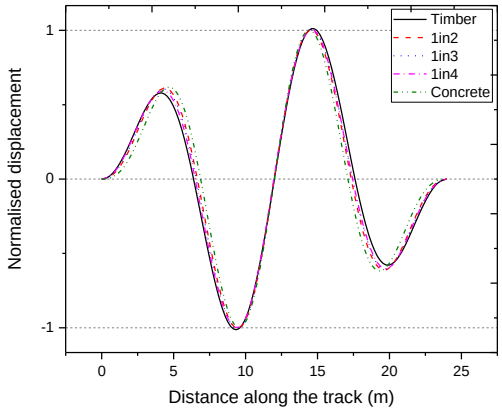
Timber
1in2
1in3
1in4
Concrete
Normalised displacement
Distance along the track (m)

g)

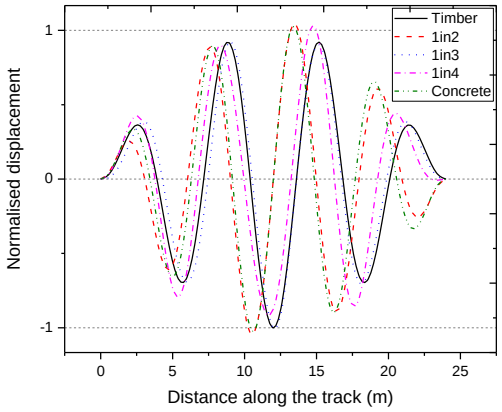
Timber
1in2
1in3
1in4
Concrete
Normalised displacement
Distance along the track (m)

h)

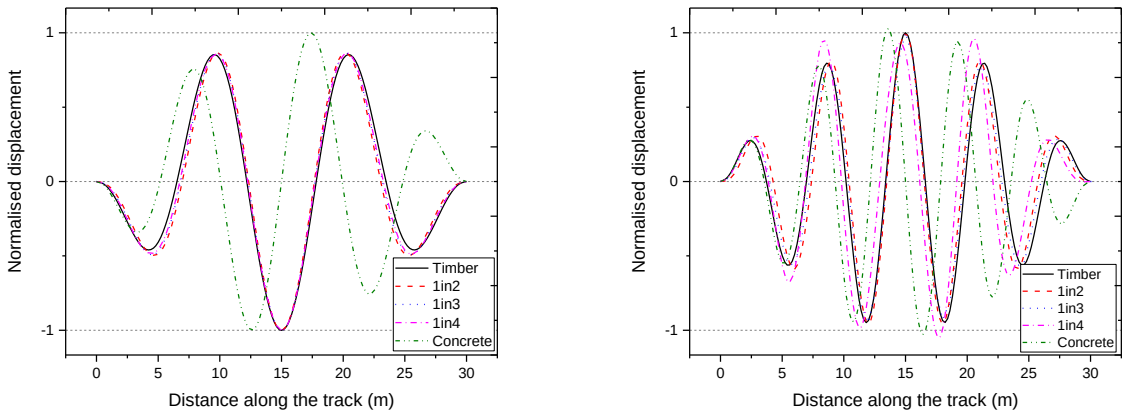

Figure 6 Buckling shape of railway tracks with different conditions:
a) Unconstrained length = 6m, Lateral stiffness = 200N/mm
b) Unconstrained length = 6m, Lateral stiffness = 2000N/mm
c) Unconstrained length = 12m, Lateral stiffness = 200N/mm
d) Unconstrained length = 12m, Lateral stiffness = 2000N/mm
e) Unconstrained length = 18m, Lateral stiffness = 200N/mm
f) Unconstrained length = 18m, Lateral stiffness = 2000N/mm
g) Unconstrained length = 24m, Lateral stiffness = 200N/mm
h) Unconstrained length = 24m, Lateral stiffness = 2000N/mm
i) Unconstrained length = 30m, Lateral stiffness = 200N/mm
j) Unconstrained length = 30m, Lateral stiffness = 2000N/mm

Fig 7 presents the effects of unconstrained length on buckling temperature. It is clear that the larger unconstrained length can buckle the tracks earlier in comparison to the shorter unconstrained length due to their higher slenderness ratio. As for the 6m unconstrained length of tracks that can be defined as similar as short column, the buckling temperature for all tracks is much larger than others as it requires larger load to buckle the track. For tracks with over 12m unconstrained length, the buckling temperature is slightly affected by the boundary conditions. The buckling temperature tends to be reduced constantly when the unconstrained length reaches the certain length. It is obvious that railway tracks can be buckled when subjected to the same temperature level when the unconstrained length is over 24m. As for the buckling temperature in general, concrete sleepered track demonstrates the best buckling prevention performance, resulting in higher buckling temperature. In terms of the interspersed railway tracks, the 1in2 track has better performance than 1in3 and 1in4 due to the higher number of concrete sleepers that have higher lateral stiffness than timber sleepers. However, when the track stiffness is 200N/mm, the reverse result is shown: concrete sleepered track is worse than other tracks as the rotation stiffness of the fastening system of concrete sleepers is one third of that of timber sleeper and the lateral stiffness does not help to track to prevent buckling. Thus, the unconstrained length of 30m of railway tracks is chosen for nonlinear analysis to analyse the buckling temperature.

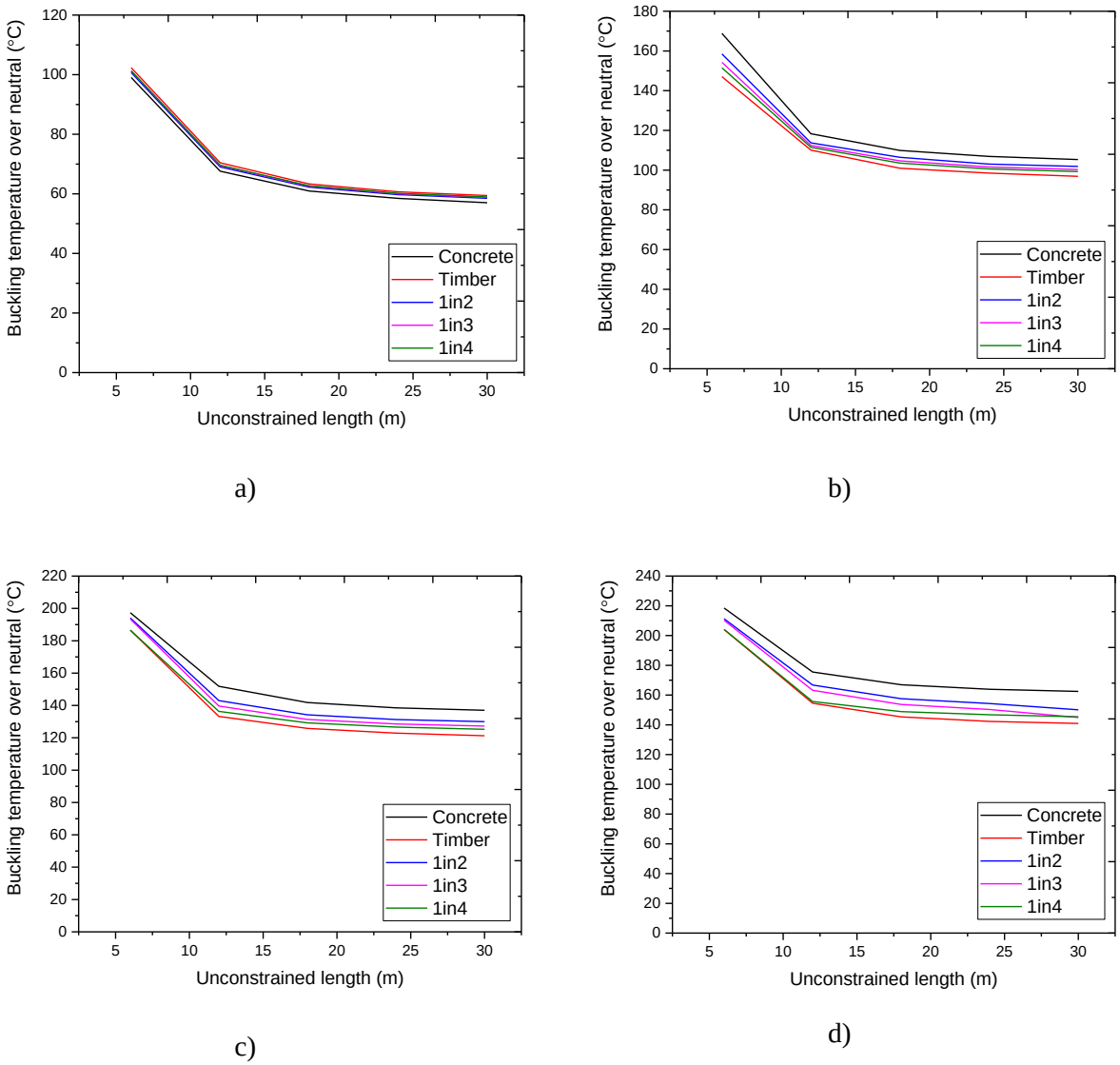

Figure 7 Buckling temperature over neutral and unconstrained length of railway tracks with lateral stiffness of a) 200N/mm b) 800 N/mm c) 1400 N/mm d) 2000N/mm.

Fig 8 presents the buckling temperature rise above neutral temperature considering the unconstrained length, lateral stiffness and torsional stiffness. It should be noted that the lower and upper bounds of torsional resistance are the nominal values times 0.5 and 1.5, respectively. These are represented as the effects of torsional fastening resistance by dot and dash lines in Fig 8. It is clear that lateral stiffness plays a very significant role while the torsional fastening resistance plays a slight role in improving the buckling resistance. All tracks show similar trends in term of lateral resistance. However, it is observed that the torsional fastening resistance in concrete sleepered track hardly influences the buckling temperature while the fastening systems can potentially help timber sleepered track to improve the buckling resistance as seen in the wider range between the upper and lower bounds of buckling temperature.

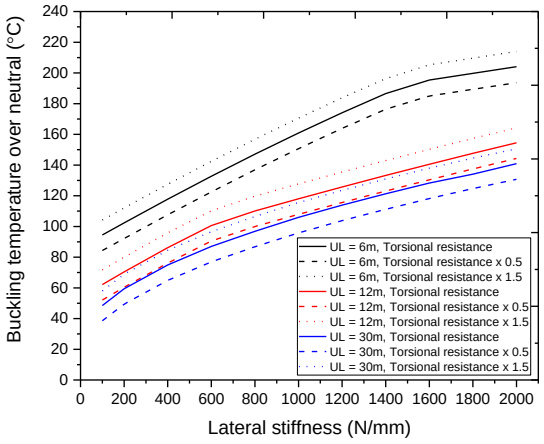
Buckling temperature over neutral (°C)
Lateral stiffness (N/mm)
UL = 6m, Torsional resistance
UL = 6m, Torsional resistance x 0.5
UL = 6m, Torsional resistance x 1.5
UL = 12m, Torsional resistance
UL = 12m, Torsional resistance x 0.5
UL = 12m, Torsional resistance x 1.5
UL = 30m, Torsional resistance
UL = 30m, Torsional resistance x 0.5
UL = 30m, Torsional resistance x 1.5

a)

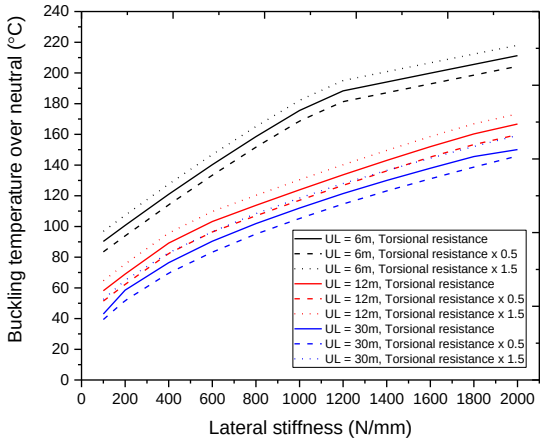
Buckling temperature over neutral (°C)
Lateral stiffness (N/mm)
UL = 6m, Torsional resistance
UL = 6m, Torsional resistance x 0.5
UL = 6m, Torsional resistance x 1.5
UL = 12m, Torsional resistance
UL = 12m, Torsional resistance x 0.5
UL = 12m, Torsional resistance x 1.5
UL = 30m, Torsional resistance
UL = 30m, Torsional resistance x 0.5
UL = 30m, Torsional resistance x 1.5

b)

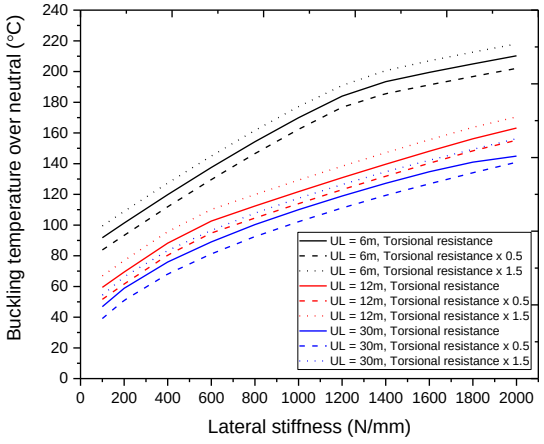
Buckling temperature over neutral (°C)
Lateral stiffness (N/mm)
UL = 6m, Torsional resistance
UL = 6m, Torsional resistance x 0.5
UL = 6m, Torsional resistance x 1.5
UL = 12m, Torsional resistance
UL = 12m, Torsional resistance x 0.5
UL = 12m, Torsional resistance x 1.5
UL = 30m, Torsional resistance
UL = 30m, Torsional resistance x 0.5
UL = 30m, Torsional resistance x 1.5

c)

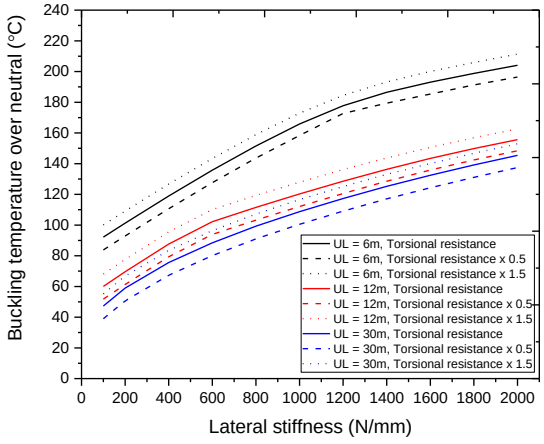
Buckling temperature over neutral (°C)
Lateral stiffness (N/mm)
UL = 6m, Torsional resistance
UL = 6m, Torsional resistance x 0.5
UL = 6m, Torsional resistance x 1.5
UL = 12m, Torsional resistance
UL = 12m, Torsional resistance x 0.5
UL = 12m, Torsional resistance x 1.5
UL = 30m, Torsional resistance
UL = 30m, Torsional resistance x 0.5
UL = 30m, Torsional resistance x 1.5

d)

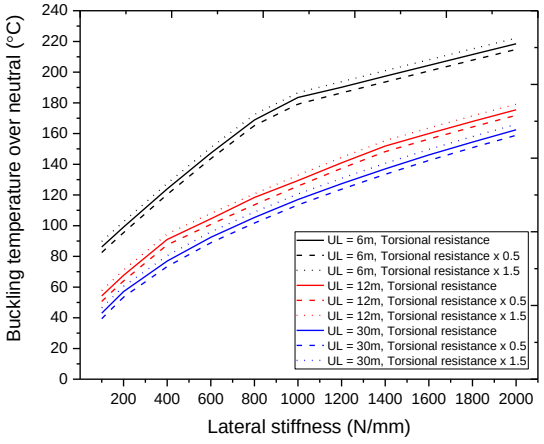
Buckling temperature over neutral (°C)
Lateral stiffness (N/mm)
UL = 6m, Torsional resistance
UL = 6m, Torsional resistance x 0.5
UL = 6m, Torsional resistance x 1.5
UL = 12m, Torsional resistance
UL = 12m, Torsional resistance x 0.5
UL = 12m, Torsional resistance x 1.5
UL = 30m, Torsional resistance
UL = 30m, Torsional resistance x 0.5
UL = 30m, Torsional resistance x 1.5

e)

Figure 8 Effects of ballast lateral and fastening torsional resistance of a) Timber sleepered track b) 1in2 interspersed track c) 1in3 interspersed track d) 1in4 interspersed track e) Concrete sleepered track.

5.2 Nonlinear analysis

This study analyses the rail axial force induced by the change in rail temperature. To understand the physical behaviour of railway track buckling, the buckling failure mode should be investigated together with rail axial force that can be seen from the relationship between rail axial force and temperature rise above neutral. Fig 9 presents the rail axial force of timber and concrete sleepered tracks exposed to the temperature rise above neutral temperature. The cases presented are when the lateral stiffness has 1mm displacement limit. Note that the shape of initial misalignment is the first symmetrical buckling shape derived from linear analysis (Fig 6a) which is the most critical and likely to occur. The initial misalignment amplitude varies from 8mm to 32mm.

The rail axial force-temperature relationships are presented in Fig 9. During the first stage or pre-buckling, the track is stable and has a very small lateral displacement due to the lateral restraint. The axial force increases due to the thermal expansion. The buckling temperature is measured when the axial compression reaches the buckling resistance as can be seen at the maximum temperature. The critical buckling force represents the maximum compressive axial force that the railway track can sustain due to an increase in rail temperature. After this point, it is important to note that railway tracks undergo a large lateral deformation accompanied by axial contraction. The reduction in axial load is observed after reaching the buckling temperature. However, in the post buckling stage, the reduction in axial load can occur in different scenarios depending on track conditions. It is interesting that the axial force can be reduced progressively after buckling. This behaviour is likely to be observed in railway tracks with weaker lateral resistance such as timber sleepered tracks. It is more obvious especially when the misalignment is large and railway tracks have weak lateral stiffness (Fig 9c). This clearly represents the progressive buckling failure. Besides, the sudden reduction of rail axial force can be observed in stronger tracks. After that, the rails constantly undergo further lateral displacement. Therefore, railway tracks are generally buckled in the snap-through phenomenon. Even though track with higher lateral stiffness can effectively prevent track buckling and prolong track stability under temperature rise, tracks that are buckled by large axial force tends to have larger self-excitation after buckling. Despite snap-through buckling is an explosive shift of lateral displacement after buckling, it is clear that snap-through buckling occurs under a much greater buckling temperature or rail axial force for railway tracks with higher stiffness. Even though progressive buckling is referred to a much slower increase in lateral alignment after buckling, progressive buckling should be avoided as it usually occurs when the track has lower lateral stiffness leading to a progressive displacement even the low temperature is applied, as seen in Fig 1. The lateral displacement gradually increases under a much lower temperature compared to snap-through buckling. This increased displacement can add up to the initial misalignment leading to greater misalignment and increasing risk of train derailment.

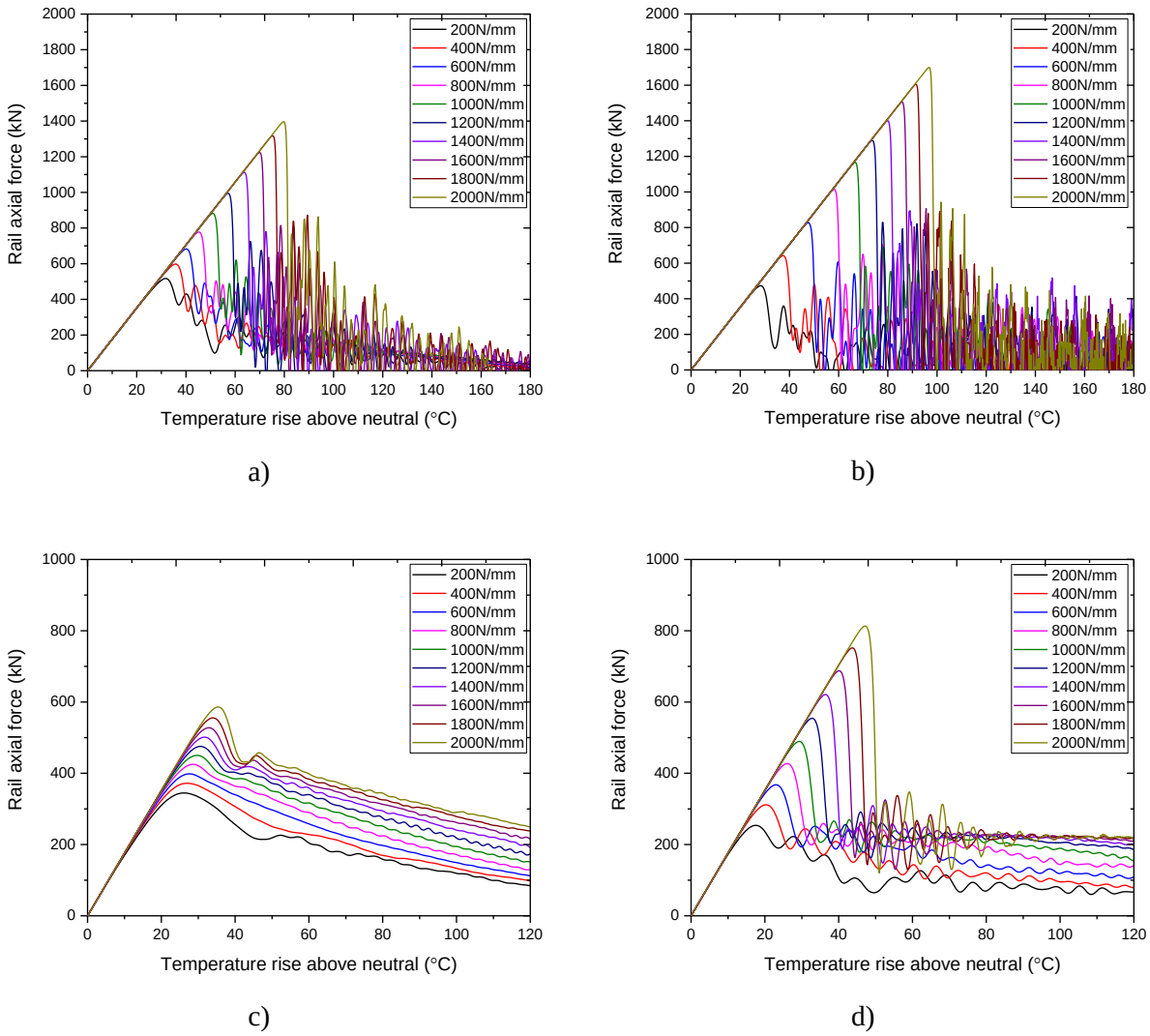

Figure 9 Axial force-temperature relationship of a) timber sleepered tracks (8mm-misalignment) b) concrete sleepered tracks (8mm-misalignment) c) timber sleepered tracks (32mm-misalignment) d) concrete sleepered tracks (32mm-misalignment).

The buckling temperatures over neutral and critical buckling axial force of railway tracks are presented in Fig 10. The 1mm and 2mm displacement limit of lateral resistance curves are compared. It should be noted that the lateral resistance shown in the horizontal axis is calculated by the lateral resistance force divided by displacement limit. It implies that the lateral resistance force for 2mm displacement limit is higher than that for 1mm displacement limit. The results show that the lateral resistance significantly improves the buckling strength for all cases. It is noted that, with the same lateral stiffness value, the higher displacement limit of the lateral resistance curve can potentially increase the buckling temperature. As for the case of 2mm displacement limit, the buckling temperature and buckling force of concrete sleepered track are the highest and followed by 1in2, 1in3 1in4 interspersed tracks and timber sleepered track, respectively. This can be clearly seen especially when the lateral stiffness is high. As for 1mm displacement limit, the buckling strength are in the similar trends to those for 2mm displacement limit case. However, the inverse trends are shown when the lateral resistance is reduced to certain values. For instance, for the tracks with a misalignment amplitude of 8mm, the inflection point is around 350 N/mm lateral stiffness. Below this point,

the timber sleepered and 1in2 interspersed track possesses greater buckling temperature than 1in3, 1in4 and concrete sleepered tracks. This is because the larger torsional fastening stiffness of timber sleepers helps track to resist buckling as the lateral stiffness can no longer help resist track buckling.

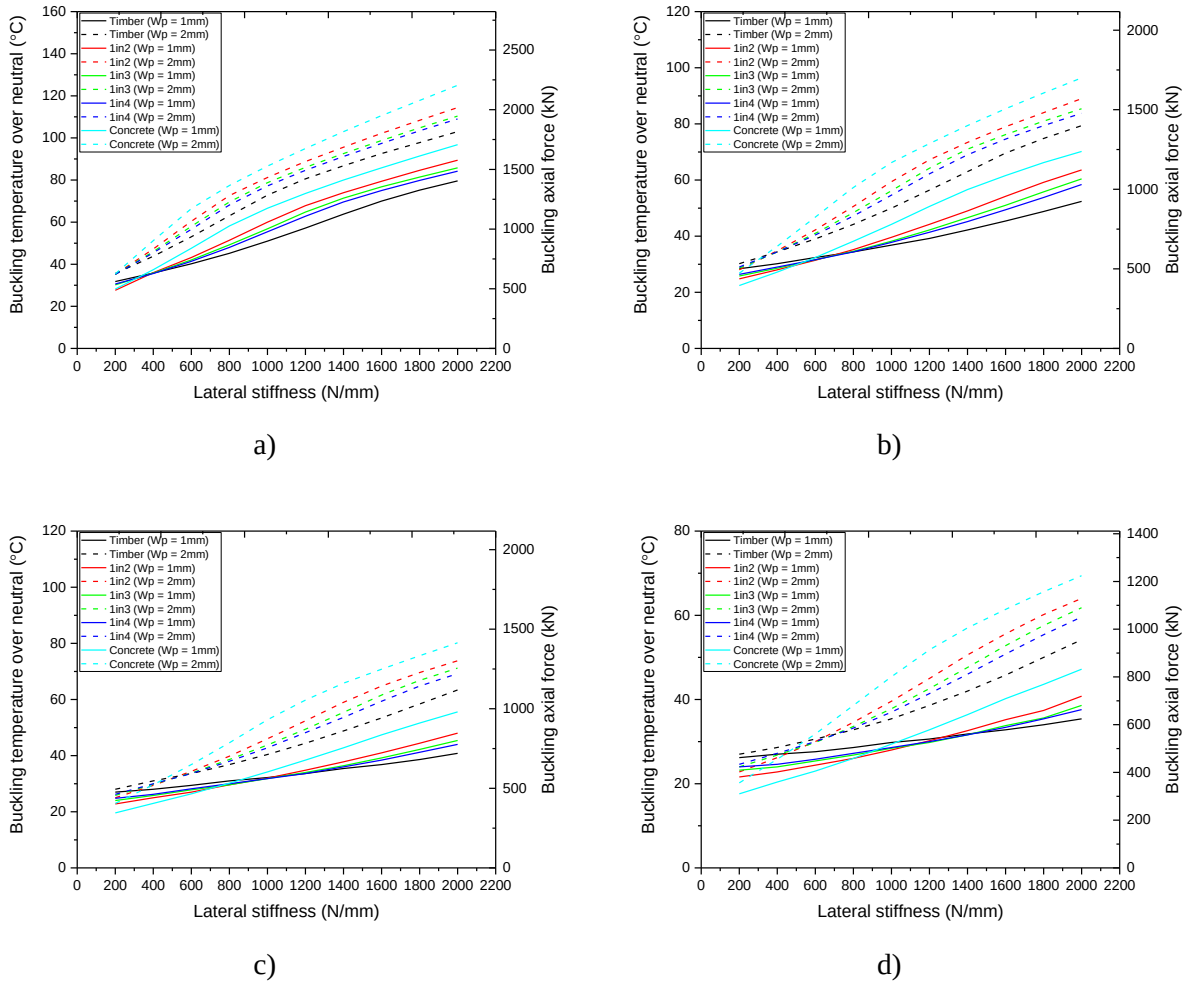

Figure 10 Buckling temperature and buckling axial force of railway tracks with lateral misalignment amplitude of a) 8mm b) 16mm c) 24mm d) 32mm.

The effects of lateral misalignments are presented in Fig 11. It can be clearly seen that, overall, buckling temperatures decrease as the misalignment amplitude increases. As for the 200N/mm lateral stiffness tracks, interspersed methods can potentially increase the buckling temperature when the misalignment amplitude is high. However, the trends are not consistent when the lateral stiffness of tracks are 200N/mm and 800N/mm (Figs 11a and 11b). When the lateral stiffness is higher (Figs 11c and 11d), the interspersed method can help significantly increase the buckling temperature even if the misalignment amplitude is either small or large. It can be concluded that when the track is more stable, the method of interspersing can significantly improve the buckling resistance. Overall, the 2mm displacement limit yields larger buckling temperature and the trends are more consistent as the lateral resistance force is higher.

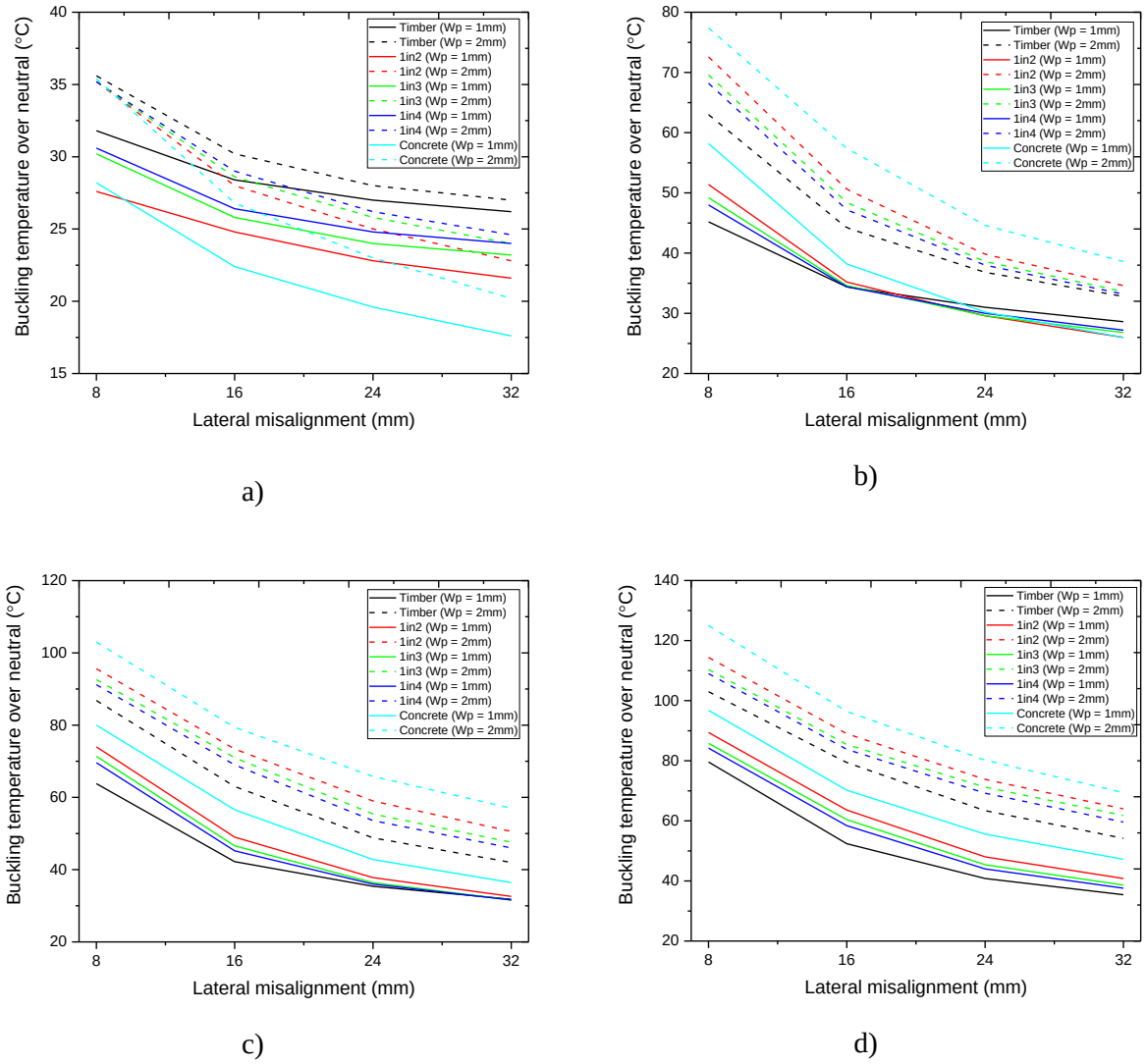

Figure 11 Effects of track lateral misalignment of railway tracks with lateral stiffness of a) 200N/mm b) 800N/mm c) 1400N/mm d) 2000N/mm.

6. Conclusions

In this study, 3D finite element models are developed to investigate the buckling behaviour of interspersed railway tracks. It should be noted that many researchers have investigated the buckling phenomena of timber sleepered and concrete sleepered tracks. However, buckling analysis of interspersed railway tracks has never been fully conducted. The main aim of the interspersed method is to replace the ageing timber sleepers by alternative materials such as concrete. It is important to note that interspersed railway tracks have issues of inconsistent stiffness and material properties. Nonetheless, interspersed tracks seem to have benefits in preventing track buckling in comparison to conventional timber sleepered tracks. The following key findings are revealed by the parametric studies and obtained results.

- The replacement of timber sleepers by concrete sleepers tends to increase the buckling temperature. This, the buckling resistance of railway tracks from high to low can be presented in order as plain concrete sleepered track, 1in2, 1in3, 1in4, and plain timber sleepered track. While

the results of safe temperature do not follow the trends of the buckling temperature results due to the influences from different factors.

- Initial lateral misalignment has a significant influence on buckling temperature. This means increasing misalignment results in buckling temperature reduction while it has less effect on safe temperature.
- The unconstrained length has an effect on the track buckling shapes which cause various defects and misalign the track.
- It is important to minimise the length of weak area and keep the tracks restrained laterally as these can significantly help increase the buckling temperature.
- In case of low lateral stiffness, the buckling trends can be reversed as the ballast can no longer help mitigate track buckling. The torsional fastening stiffness can rather help in this case and thus the timber sleepered track has higher buckling temperature than interspersed tracks.
- Replacing timber sleepers by concrete sleepers can shift the buckling failure mechanism from progressive buckling to snap-through buckling. Note that progressive buckling usually occurs when the track has less buckling strength that should be avoided due to its gradual increase in lateral displacement from a very low temperature compared to snap-through buckling.
- For unloaded tracks, despite the fact that the timber sleepered tracks might have a higher safe temperature than the interspersed and concrete sleepered tracks, the timber sleepered tracks require less buckling energy to buckle the track at the safe temperature level. This is attributed to the fact that the difference between the buckling temperature and the safe temperature is considerably less than that in the case of the interspersed and concrete sleepered tracks, showing that the timber sleepered tracks are more likely to have a progressive buckling failure than the others.

Based on the findings, the interspersed method could be an alternative cost-effective method for the ballasted tracks with pure timber sleepers to improve the buckling strength and mitigate track buckling. The insights will enhance the inspection regime for buckling strength of lateral stiffness in railway systems and mitigate the risk of delays due to unplanned maintenance, thus paving a robust pathway for a practical impact on society.

Acknowledgments

The authors are sincerely grateful to European Commission for the financial sponsorship of the H2020-MSCA-RISE Project No. 691135 “RISEN: Rail Infrastructure Systems Engineering Network,” which enables a global research network that tackles the grand challenge of railway infrastructure resilience and advanced sensing in extreme environments (www.risen2rail.eu).

References

1. Oslakovic IS, Maat HWT, Hartmann A, Dewulf G. Risk assessment of climate change impacts on railway infrastructure. 2013.
2. Quinn AD, Jack A, Hodgkinson S, Ferranti EJS, Beckford J, Dora J. Rail Adapt: Adapting the Railway for the Future. A Report for the International Union of Railways (UIC). 2017.
3. Ngamkhanong C, Kaewunruen S, Costa BJA. State-of-the-art review of railway track resilience monitoring. Infrastructures. 2018;3(1):3.
4. Ahmad SSN, Mandal NK, Chattopadhyay G. A comparative study of track buckling parameters on continuous welded rail. 2009. p. 26-8.
5. Esveld C. Modern railway track: MRT-productions Zaltbommel, Netherlands; 2001.
6. Kish A. On the fundamentals of track lateral resistance. American Railway Engineering and Maintenance of Way Association. 2011.
7. Esveld C. Improved knowledge of CWR track. 1997. p. 8-9.

8. Ling L, Xiao XB, Cao YB, Wu L, Wen Z, Jin XS, editors. Numerical simulation of dynamical derailment of high-speed train using a 3D train–track model2014.
9. Ling L, Xiao XB, Jin XS. Development of a simulation model for dynamic derailment analysis of high-speed trains. Acta Mechanica Sinica. 2014;30(6):860-75.
10. Kaewunruen S, Wang Y, Ngamkhanong C. Derailment-resistant performance of modular composite rail track slabs. Engineering Structures. 2018;160:1-11.
11. Kohoutek R, Campbell KD. Analysis of spot replacement sleepers. 1989: Institution of Engineers, Australia. p. 316.
12. Ferdous W, Manalo A, Van Erp G, Aravinthan T, Kaewunruen S, Remennikov A. Composite railway sleepers–Recent developments, challenges and future prospects. Composite Structures. 2015;134:158-68.
13. Gustavson RPG. Structural behaviour of concrete railway sleepers. 2004.
14. Kaewunruen S, Remennikov A, Aikawa A, Sakai H. Free vibrations of interspersed railway track systems in three-dimensional space. 2014.
15. Kaewunruen S, Chamniprasart K. Damage analysis of spot replacement sleepers interspersed in ballasted railway tracks. Proceedings of the 29th Nordic Seminar on Computational Mechanics; 2016; Chalmers University of Technology, Gothenburg, Sweden2014.
16. Kohoutek R. Dynamic and static performance of interspersed railway track. 1991: Institution of Engineers, Australia; 1991. p. 153.
17. Lake M, Ferreira L, Murray M. Using simulation to evaluate rail sleeper replacement alternatives. Transportation research record. 2002;1785(1):58-63.
18. Connolly DP, Kouroussis G, Laghrouche O, Ho CL, Forde MC. Benchmarking railway vibrations–Track, vehicle, ground and building effects. Construction and Building Materials. 2015;92:64-81.
19. Kaewunruen S, Remennikov AM. Experimental simulation of the railway ballast by resilient materials and its verification by modal testing. Experimental Techniques. 2008;32(4):29-35.
20. Kaewunruen S, Remennikov AM. Nonlinear transient analysis of a railway concrete sleeper in a track system. International Journal of Structural Stability and Dynamics. 2008;8(03):505-20.
21. Kaewunruen S, Ngamkhanong C, Janeliukstis R, You R. Influences of surface abrasions on dynamic behaviours of railway concrete sleepers. 2017. p. 20-4.
22. Ngamkhanong C, Li D, Kaewunruen S, editors. Impact capacity reduction in railway prestressed concrete sleepers with surface abrasions2017.
23. Ngamkhanong C, Kaewunruen S, Baniotopoulos C. A review on modelling and monitoring of railway ballast. Structural Monitoring and Maintenance. 2017;4(3):195-220.
24. Ngamkhanong C, Li D, Remennikov AM, Kaewunruen S. Dynamic capacity reduction of railway prestressed concrete sleepers due to surface abrasions considering the effects of strain rate and prestressing losses. International Journal of Structural Stability and Dynamics. 2019;19(01):1940001.
25. Kaewunruen S, Ngamkhanong C, Lim CH. Damage and failure modes of railway prestressed concrete sleepers with holes/web openings subject to impact loading conditions. Engineering Structures. 2018;176:840-8.
26. Kaewunruen S, Lewandrowski T, Chamniprasart K. Nonlinear modelling and analysis of moving train loads on interspersed railway tracks. 2018. p. 15-7.
27. Kaewunruen S, Lewandrowski T, Chamniprasart K. Dynamic responses of interspersed railway tracks to moving train loads. International Journal of Structural Stability and Dynamics. 2018;18(01):1850011.
28. Kaewunruen S, Ng J, Aikawa A. Sensitivity of rail pads on dynamic responses of spot replacement sleepers interspersed in ballasted railway tracks. Proceedings of the 25th International Congress on Sound and Vibration; 2018; Hiroshima, Japan2018. p. 8-12.
29. Kaewunruen S, Ngamkhanong C, Ng J. Influence of time-dependent material degradation on life cycle serviceability of interspersed railway tracks due to moving train loads. Engineering Structures. 2019;199:109625.

30. Zakeri JA, Bakhtiary A. Comparing lateral resistance to different types of sleeper in ballasted railway tracks. Scientia Iranica,. 2014;21(1):101-7.
31. Kish A, Clark DW, Thompson W. Recent Investigations on the Lateral Stability of Wood and Concrete Tie Tracks. AREA Bulletin. 1995;752:248-65.
32. Lichtberger B. The lateral resistance of the track (Part 2). European Railway Review. 2007.
33. Tutumluer E, Huang H, Hashash Y, Ghaboussi J, editors. Aggregate shape effects on ballast tamping and railroad track lateral stability. AREMA 2006 Annual Conference; September 17-20, 2006; Louisville, KY, USA2006.
34. Jing G, Aela P, Fu H. The contribution of ballast layer components to the lateral resistance of ladder sleeper track. Construction and Building Materials. 2019;202:796-805.
35. Guo Y, Fu H, Qian Y, Markine V, Jing G. Effect of sleeper bottom texture on lateral resistance with discrete element modelling. Construction and Building Materials. 2020;250.
36. Jing G, Aela P, Fu H, Yin H. Numerical and experimental analysis of single tie push tests on different shapes of concrete sleepers in ballasted tracks. Proceedings of the Institution of Mechanical Engineers, Part F: Journal of Rail and Rapid Transit. 2018;233(7):666-77.
37. Prud'Homme MA, Janin MG. The stability of tracks laid with long welded rails. RAIL INTERNATIONAL. 1969;46:459-87.
38. Kerr AD. Analysis of thermal track buckling in the lateral plane. Acta Mechanica. 1978;30(1-2):17-50.
39. Kerr AD. An improved analysis for thermal track buckling. International Journal of Non-Linear Mechanics. 1980;15(2):99-114.
40. Samavedam G, Kish A, Purple A, Schoengart J. Parametric Analysis and Safety Concepts of CWR Track Buckling. United States. Federal Railroad Administration; 1993.
41. Sussmann T, Kish A, Trosino M. Influence of track maintenance on lateral resistance of concrete-tie track. Transportation research record. 2003;1825(1):56-63.
42. Ole ZK. Track stability and buckling-rail stress management. Australia: Unversity of Southern Queensland; 2008.
43. Carvalho J, Delgado J, Calcada R, Delgado R. A new methodology for evaluating the safe temperature in continuous welded rail tracks. International Journal of Structural Stability and Dynamics. 2013;13(02):1350016.
44. Cuadrado M, Zamorano C, González P, Nasarre J, Romo E. Analysis of buckling in dual-gauge tracks. Proceedings of the Institution of Civil Engineers-Transport. 2008;161:177-84.
45. Villalba I, Insa R, Salvador P, Martinez P. Methodology for evaluating thermal track buckling in dual gauge tracks with continuous welded rail. Proceedings of the Institution of Mechanical Engineers, Part F: Journal of Rail and Rapid Transit. 2017;231(3):269-79.
46. Villalba Sanchis I, Insa R, Salvador P, Martínez P. An analytical model for the prediction of thermal track buckling in dual gauge tracks. Proceedings of the Institution of Mechanical Engineers, Part F: Journal of Rail and Rapid Transit. 2018;232(8):2163-72.
47. Ngamkhanong C, Wey CM, Kaewunruen S. Buckling Analysis of Interspersed Railway Tracks. Appl Sci. 2020;10:3091.
48. Cai Z. Modelling of rail track dynamics and wheel/rail interaction. Kingston, ON, Canada: Queen's University; 1994.
49. Zakeri JA, Mirfattahi B, Fakhari M, editors. Lateral resistance of railway track with frictional sleepers2012: Thomas Telford Ltd.
50. El-Ghazaly HA, Sherbourne AN, Arbabi F. Strength and stability of railway tracks—II Deterministic, finite element stability analysis. Computers & structures. 1991;39(1-2):23-45.
51. Yang G, Bradford MA. Thermal-induced buckling and postbuckling analysis of continuous railway tracks. International Journal of Solids and Structures. 2016;97:637-49.
52. CRC for Rail Innovation. Track Stability Management – Literature Review: Theories and Practices Brisbane, Australia: CRC for Rail Innovation 2009. Contract No.: R3.112

53. Federal Railroad Administration (FRA). Continuous welded rail (CWR); general. Federal Railroad Administration (FRA); 2010. Contract No.: Sec. 213.119.